

REPORT DOCUMENTATION PAGE

Form Approved
OMB No. 0704-0188

Public reporting burden for this collection of information is estimated to average 1 hour per response, including the time for reviewing instructions, searching existing data sources, gathering and maintaining the data needed, and completing and reviewing the collection of information. Send comments regarding this burden estimate or any other aspect of this collection of information, including suggestions for reducing this burden, to Washington Headquarters Services, Directorate for Information Operations and Reports, 1215 Jefferson Davis Highway, Suite 1204, Arlington, VA 22202-4302, and to the Office of Management and Budget, Paperwork Reduction Project (0704-0188), Washington, DC 20503.

1. AGENCY USE ONLY (Leave blank)		2. REPORT DATE 12/25/1996	3. REPORT TYPE AND DATES COVERED 9/30/92- Final Technical Report, 10/31/96	
4. TITLE AND SUBTITLE Spectroscopy of Metal-Hydrogen Clusters			5. FUNDING NUMBERS F49620-92-J-0537 61102F 2303 ES	
6. AUTHOR(S) Mitchio Okumura				
7. PERFORMING ORGANIZATION NAME(S) AND ADDRESS(ES) Chemistry Department 127-72 California Institute of Technology 1200 East California Blvd. Pasadena, CA 91125			AFOSR-TR-97 0069	
9. SPONSORING/MONITORING AGENCY NAME(S) AND ADDRESS(ES) Dr. Michael Berman, Program Manager AFOSR/NL 110 Duncan Avenue Suite B115 Bolling AFB DC 20332-0001			10. SPONSORING/MONITORING AGENCY REPORT NUMBER F49620-92-J-0537	
11. SUPPLEMENTARY NOTES			19970131 058	
12a. DISTRIBUTION/AVAILABILITY STATEMENT Approved for public release; distribution unlimited.			12b. DISTRIBUTION CODE	
13. ABSTRACT (Maximum 200 words) Spectroscopic studies of clusters have been carried out in order to aid in the investigation of metal atom doping of solid hydrogen as a possible High Energy Density Material. The electronic spectra of small metal-atom clusters provides a well defined system for understanding the intermolecular forces between guest atoms and hosts and offers a stringent test of theoretical methods. In this work, a cluster beam spectroscopy apparatus was constructed to obtain spectra of clusters by laser-induced fluorescence and resonant multiphoton ionization. Electronic spectra were recorded for roughly size-selected clusters containing Al atoms bound to Ar clusters (containing up to 55 Ar atoms) by two photon ionization spectroscopy. The variations in band shifts and splittings provide an important measure of both cluster structure and perturbations of the atomic transitions. Efforts are now underway at Phillips Laboratory to test theoretical models of atom doping by comparing computed spectra with those reported here. In addition, laser-induced fluorescence spectra were observed and tentatively assigned to AlNe and Al-water.				
14. SUBJECT TERMS			15. NUMBER OF PAGES 33	
			16. PRICE CODE	
17. SECURITY CLASSIFICATION OF REPORT u	18. SECURITY CLASSIFICATION OF THIS PAGE u	19. SECURITY CLASSIFICATION OF ABSTRACT u	20. LIMITATION OF ABSTRACT u	

Spectroscopy of Metal-Hydrogen Clusters

Mitchio Okumura

Arthur Amos Noyes Laboratory of Chemical Physics

Mail Code 127-72

California Institute of Technology

1200 East California Blvd.

Pasadena, CA 91125

I. Summary

A. INTRODUCTION

1. Motivation and Air Force Interests. The High Energy Density Matter (HEDM) program has identified atom-doped solid hydrogen as a high energy molecular system with promise as an alternative rocket propellant that can provide significant improvements in specific impulse (I_{sp}) over conventional propulsion technology. Calculations indicate that doping of light metal atoms as well as their dimers can yield increases in I_{sp} 's of several percent at reasonable doping concentrations. Critical issues in scaleup and engineering remain to be addressed. Modeling of the structure and dynamics of these systems at the molecular level provide a fundamental basis for efforts to develop these materials as viable propellant systems.

Matrix spectroscopy is one of the most important probes of the physical environment around a dopant atom. A key uncertainty in matrix studies underway at Phillips Laboratory, Edwards AFB, lies in the interpretation of the matrix-induced shifts and splittings of atomic spectral transitions. Such experiments must ultimately rely on high level calculations to correctly predict the splittings and shifts expected. The theory must accurately compute two

properties: the structure of the matrix and the perturbations induced by the matrix on the electronic spectrum of the dopant atom. Additional uncertainties such as multiple trapping sites further complicate the analysis of matrix spectra.

High resolution spectroscopy of clusters provides a far simpler means of exploring the potential energy surfaces that govern the dynamics in the condensed phase. The intermolecular forces in solid hydrogen and in inert rare gas matrices are weak and can be precisely probed in spectroscopic studies of small clusters of a single dopant atom (or molecule) complexed with inert rare gas atoms (e.g. Ar) and H₂ molecules. Furthermore, the small size of the systems provides a relatively tractable system for theoretical modeling. Investigations of clusters can thus provide detailed information concerning the interaction between a metal dopant and the surrounding hosts, the fundamental data necessary to accurately model the behavior of a guest dopant metal with a surrounding host hydrogen matrix. Most importantly, the results of specific cluster studies also serve as rigorous tests of the theoretical methods that are being developed at Phillips Laboratory to calculate the properties of solid H₂ and other HEDM material.

2. Objectives. Our goal has been to investigate the spectroscopy of clusters in order to understand the guest-host interactions that exists between metal atoms doped in solid molecular and atomic matrices and the surrounding host atoms/molecules.

Two sets of experiments have been initiated. In the first, spectroscopic studies have been performed at Caltech to address directly the issue of how the electronic transitions of atoms bound to clusters and the cluster structure around the dopant evolve as a function of cluster size; these experiments have focused on a model system Al(Ar)_n. The results that we have obtained can be directly compared to calculations and thus should provide stringent

benchmarks for theoretical efforts to interpret observed matrix spectra. The second set of experiments have been undertaken to characterize two body interactions by obtaining spectra of weakly bound dimer adducts. Preliminary results have been obtained on the very weakly bound dimer adduct AlNe.

B. COMPLETED TASKS

1. Instrumentation Developed. A molecular beam spectroscopy apparatus was constructed to perform both laser-induced fluorescence and multiphoton ionization spectroscopy of metal-hydrogen clusters. A supersonic expansion/laser ablation source with cryogenic cooling capabilities was constructed to allow generation of clusters at low source temperatures.

2. MPI Spectroscopy of Aluminum-Argon Clusters. The ultraviolet spectra of $\text{Al}(\text{Ar})_n$ clusters were investigated to gain insight into the frequency shifts and band assignments of transitions observed for metal atoms trapped in cryogenic matrices. Our approach, 1+1' resonant two-color multiphoton ionization spectroscopy, allowed us to explore how the structure and ultraviolet spectra evolved with cluster size. Three bands were observed around the Al atom 3p→3d transition in the spectra of the $\text{Al}(\text{Ar})_n$ clusters. All three of these bands exhibited frequency shifts that were strongly dependent upon the degree of solvation. Data collection has been completed and a manuscript will be submitted to a refereed chemical physics journal in the near future.

3. LIF Spectroscopy of Aluminum-Neon Dimer. The electronic spectrum of the weakly bound adduct AlNe was recorded by laser-induced fluorescence spectroscopy in the region of the Al atom 3p→3d transition. This molecule is the most weakly bound Al-

complex yet observed. We have tentatively assigned the observed spectrum to progressions in the $X^2\Pi \rightarrow ^2\Delta$ transition.

3. Possible LIF Spectrum of Aluminum-H₂O Dimer. LIF spectra were recorded for Al ablation in an expansion of Ar and H₂O to search of the electronic spectrum of the Al(H₂O) complex. A series of complex progressions were observed near 300 nm, with progressions corresponding to harmonic frequencies of 122.3, 117.7, and 106.6 cm⁻¹. Because of the potential for reaction either in the ground or excited state and the absence of any matrix isolation spectra, assignment of these bands to the Al(H₂O) complex cannot be made until further studies by REMPI, allowing for mass-analysis, are performed.

C. PERSONNEL AND PUBLICATIONS

1. Personnel Participating in Research:

- a. Principal Investigator: Mitchio Okumura
- b. Graduate Students: Matthew S. Johnson, James Michael Spotts, Chi-Kin Wong, Keith T. Kuwata
- c. Undergraduates: Gary T. Olsen, Prakash Jothee, Carolyn Cohran
(Minority Undergraduate Research Fellow)

2. Publication of Results

- a. Ph.D. Thesis: Matthew S. Johnson, 1995.

“Spectroscopy of Reactive Molecules and Clusters”

California Institute of Technology, Pasadena, CA 91125.

This thesis presents detailed construction of the LIF part of the apparatus. Results are presented for the LIF spectroscopy of $\text{Al}(\text{H}_2\text{O})$. A tentative assignment of the progressions observed near 300 nm is presented.

This thesis can be obtained through the Department of Chemistry, California Institute of Technology, 164-30, 1200 E. California Blvd., Pasadena, CA 91125, as well as the Xerox Microfilm Library.

b. "REMPI Spectroscopy of AlAr_n " J. M. Spotts, Chi-Kin Wong, Matthew S. Johnson and Mitchio Okumura

A manuscript has been prepared and will be submitted to a refereed journal. Much of the text is reproduced in Section III of this report.

3. Interactions with Phillips Laboratory. We have visited both Edwards AFB and Hanscom AFB several times during the performance period. Among the most concrete results are the start of a collaboration with Drs. Jeffrey Sheehy and Jerry Boatz at Edwards AFB now underway to assign the spectra through theoretical predictions of spectra for different cluster geometries. We have also been discussing other cluster spectroscopy and metal-atom chemistry experiments with Drs. Rainer Dressler and Edmond Murad at Hanscom AFB.

II. Photoionization/LIF Apparatus

A. DESCRIPTION OF APPARATUS

A schematic of the apparatus constructed during this performance period is shown in Figure 1. It consists of a vacuum chamber with three stages of differential pumping. Region 1 is pumped by two baffled VHS-10 diffusion pumps; region 2 is pumped by a cryotrapped VHS-6 diffusion pump. Region 3 has provisions for additional pumping but is currently not differentially pumped.

In the first chamber is the molecular beam source, a piezo-electric-driven pulsed valve based on the design of Proch and Trichl (see Figure 2).¹ Clusters such as $\text{Al}(\text{Ar})_n$ were generated by laser vaporization of a target rod at 355 nm (from a tripled Continuum Surelite II Nd:YAG laser) near the exit region of the source with clustering of carrier gas to the metal atoms occurring during the ensuing supersonic expansion.

We have experimented with several versions of the nozzle/vaporization geometry, as illustrated in Figures 2 and 3. A balance is needed between the high pressure conditions needed for cluster formation and the need to maximize atomic Al (as opposed to higher metal clusters Al_n). We find that versions 2 and 3 seem to be the best source for generating $\text{Al}(\text{Ar})_n$ clusters. The laser vaporization region could also be cooled to cryogenic temperatures (77 K) using the nozzle extension shown in Figure 4, following similar adaptations built at Berkeley.² The piezo-electric element can only operate at temperatures above 273 K. To cool the nozzle further, the shaft and body were extended approximately 8 cm from the piezo-element. The seal was made with a Kel-F tip pressed against a highly polished surface. The main body of the source could thus be kept at room

temperature, with the tip (and hence final stagnation volume) cooled to liquid nitrogen temperature. The extension provided a long distance over which a thermal gradient could be established.

The UV probe laser can be introduced into either region 1 or region 2 for spectroscopic studies. Region 1 contains the optics for collecting laser-induced fluorescence. For photoionization experiments, the expansion is collimated by a 3 mm skimmer. The beam is ionized by photons from a YAG-pumped dye laser (Continuum NY-61 pumping a TDL-51 dye laser). The dye laser output can be doubled or mixed to generate ultraviolet radiation with 1-10 mJ of energy depending on wavelength. Photoions are extracted with ion optics configured in a Wiley-McLaren design.³

Region 3 contains the 1-m flight path of the time-of-flight mass spectrometer and Galileo FTD-2003 microchannel plate detector. A mass-gate has also been installed to allow for gating the mass of interest. TOF mass spectra were collected by a transient digitizer (LeCroy 8818). Individual scans were recorded by gating the mass peak of interest with a gated integrator. Both LIF and photoionization spectra were recorded with dual gated integrators (Stanford Research Systems). All spectra were normalized for laser fluence.

B. REFERENCES

¹ D. Proch and T. Trichl, Rev. Sci. Instrum. **60**, 713 (1989).

² R. E. Continetti, Ph.D. Thesis, University of California, Berkeley, CA, 1989.

³ W. C. Wiley and I. H. McLaren, Rev. Sci. Instrum. **26**, 1150 (1955).

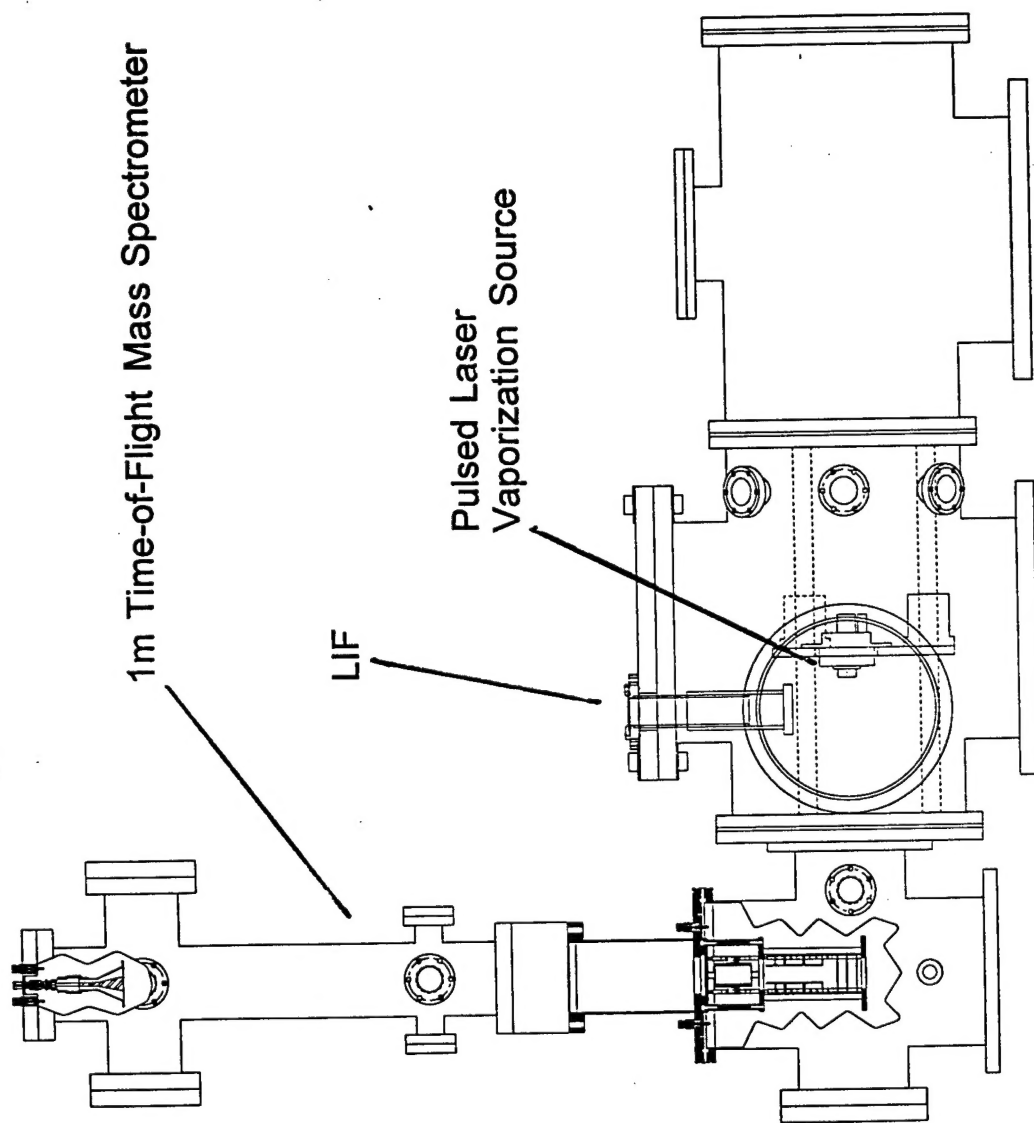


Figure 1. Photoionization/Laser -induced fluorescence spectroscopy apparatus.

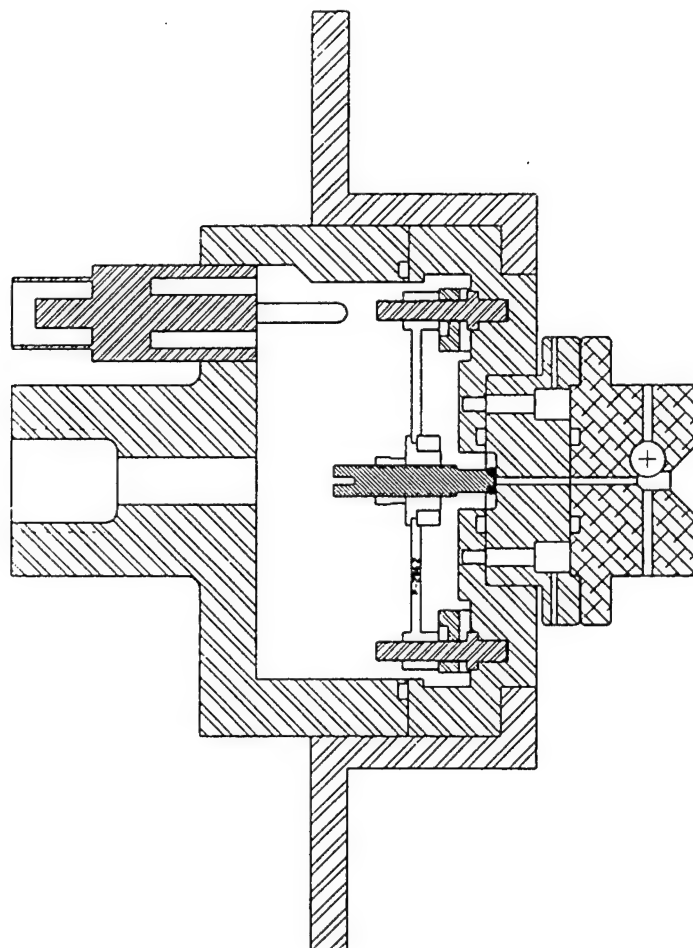


Figure 2. Pulsed valve with laser vaporization assembly.

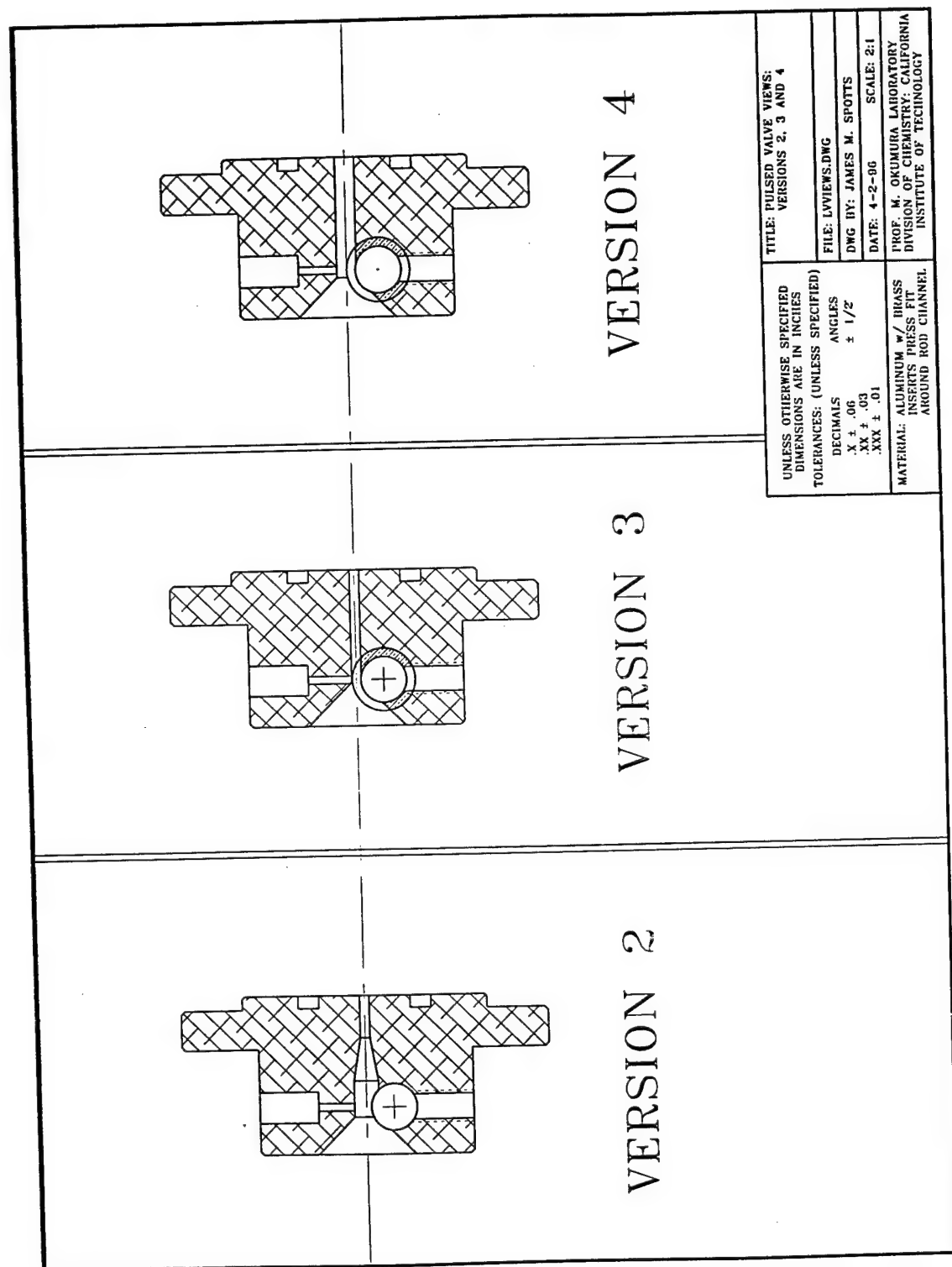


Figure 3. Variations of laser vaporization source tested for generation of metal-atom and metal-molecule clusters.

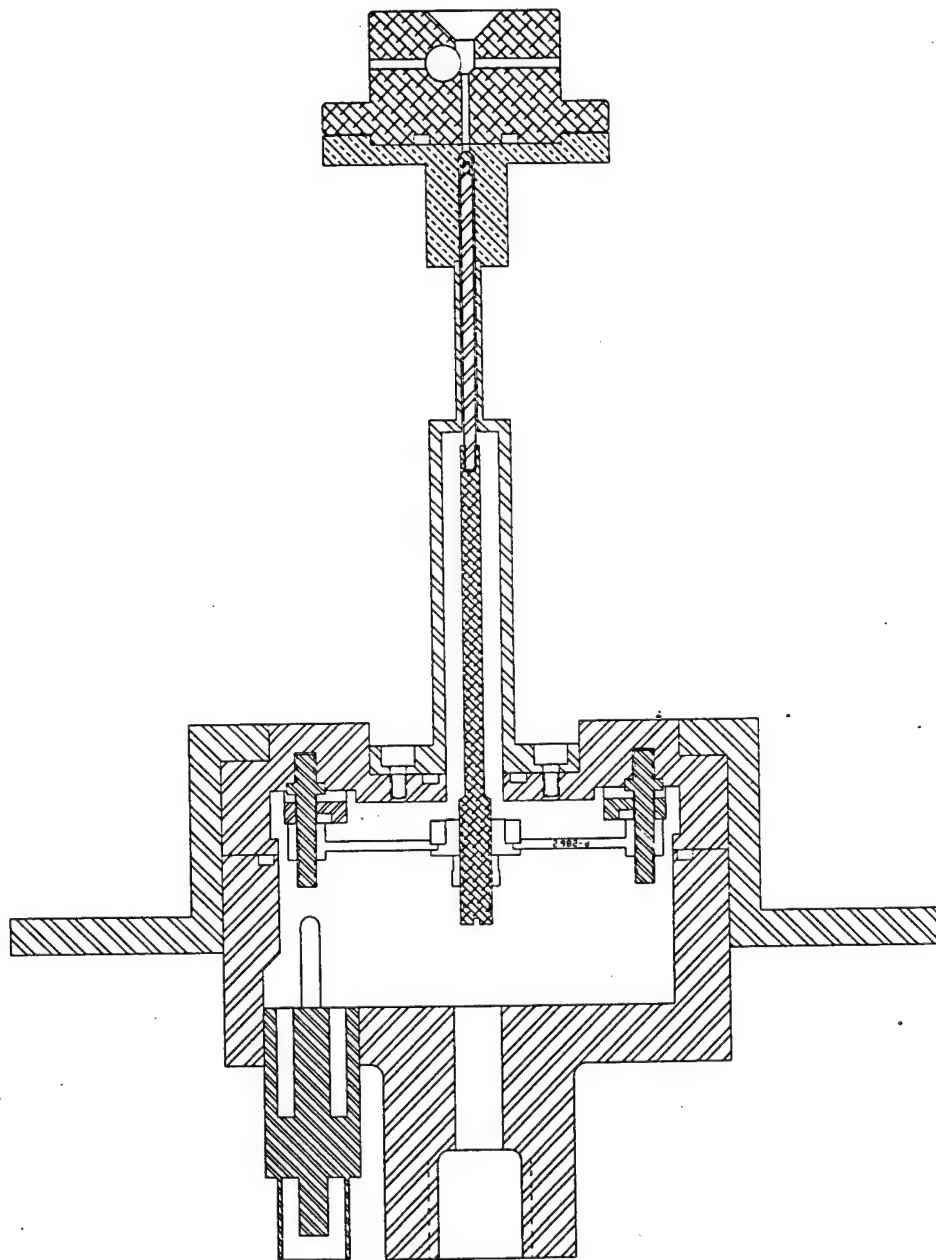


Figure 4. Cryogenically cooled pulsed valve/laser vaporization source.

III. Resonant Multiphoton Ionization Spectroscopy of $\text{Al}(\text{Ar})_n$ Clusters

The ultraviolet spectra of $\text{Al}(\text{Ar})_n$ clusters were investigated to gain insight into the frequency shifts and band assignments of transitions observed for metal atoms trapped in cryogenic matrices. Our approach, 1+1' resonant two-color multiphoton ionization spectroscopy, allowed us to explore how the structure and ultraviolet spectra evolved with cluster size. Three bands were observed around the Al atom $3p \rightarrow 3d$ transition in the spectra of the $\text{Al}(\text{Ar})_n$ clusters. All three of these bands exhibited frequency shifts that were strongly dependent upon the degree of solvation.

A. INTRODUCTION

Previous HEDM studies have predicted that the propellant properties of solid molecular hydrogen can be greatly enhanced by doping Group III atoms such as boron and aluminum into the cryogenic matrix.¹ The properties of doped matrices have been examined extensively by optical spectroscopy, but quantitative analysis in terms of lattice site, Jahn-Teller dynamics, etc. requires highly accurate theory. Recent theoretical models developed within the HEDM program have made great progress in their predictive ability to model the bonding interactions, global structure, electronic spectra, and dynamics of these and related systems. Whereas there exists some ambiguity in the interpretation of bulk systems, a reservoir of accurate, predictive information has accumulated regarding the behavior of sequentially solvated atoms or dopant atoms embedded within finite-sized clusters. As a result, we have pursued a systematic spectroscopic study of aluminum atoms solvated by Ar_n ($n < 55$). Using such a cluster approach, we sought to gain insight into the size dependent behavior of both cluster structure and the electronic band frequency shifts resulting from sequential solvation. Such measurements can provide a

stringent benchmark for testing the accuracy and reliability of the theories used to describe the bulk doped matrices.

The UV absorption spectrum of aluminum trapped in argon matrices has been extensively investigated,^{2,3} along with a number of other HEDM related systems.⁴ One such spectrum is shown in Figure 1. These studies have concentrated on the spectral region corresponding to the lowest energy Al transitions between 400-240 nm where the matrix bands appear relatively uncongested and therefore assignable. One band of interest is the matrix band assigned to the lowest energy Al transition, namely the $3p \rightarrow 4s$. While the Al $3p \rightarrow 4s$ transition appears at 395 nm, the matrix band assigned to result from the $3p \rightarrow 4s$ transition exhibits a blue shift to roughly 340 nm. Such a large blue shift is rather unusual, and the exact interactions that give rise to this shift are still unquantified. The next band, a multiplet near 290 nm has been assigned to the $3p \rightarrow 3d$ transition that occurs at 308 nm in the isolated atom.

Size-selective studies of $\text{Metal}(\text{Solvent})_n$ clusters can elucidate the interactions involved in matrix band shifts, but such measurements have rarely been undertaken. Recent experiments on alkali and alkaline earth metals solvated by He_n and Ar_n respectively have focused on very large clusters ($n \sim 100 \rightarrow >10,000$).^{5,6} In addition, Whetten and co-workers have studied the $\text{Al}(\text{Ar})_n$ cluster ($n < 150$) $3p \rightarrow 4s$ frequency shifts as a function of increasing solvation.⁷ However, these authors were unable to infer structural details from merely the solvent shifts. Far more insight could potentially be gained by investigating the matrix band spectral shifts arising from the Al ground state $3p$ manifold to the excited $3d$ manifold because asymmetries in the Al atom binding site could lift the five-fold degeneracy of the $3d$ states, leading to the possibility of more than one

resolvable band. By studying the size dependent frequency shifts and band splittings arising from transitions to the $3d$ manifold, a more complete picture of structure evolution may be inferred. For this reason, we have investigated the UV spectra of $\text{Al}(\text{Ar})_n$ clusters ($n < 56$) about the atomic aluminum $3p \rightarrow 3d$ transitions by $1+1'$ resonant two-color multiphoton ionization spectroscopy (R2MPI).

B. EXPERIMENTAL

Details of the apparatus are presented in Section II of this report. $\text{Al}(\text{Ar})_n$ clusters were generated by a standard laser vaporization techniques. Following the opening of a piezoelectric pulsed valve, the pure Ar carrier gas (~ 8 atm. stagnation pressure) entered the first of three regions of the laser vaporization source (Figure 1 of Section II). The first region consisted of a $\text{Ø}0.040''$ channel that then opened up at 10° in region 2 to join region 3, a straight $\text{Ø}0.100''$ channel. The tripled output of a Nd-YAG laser (Continuum Surelite 1) was focused on the surface of a rotatable 2024 Al rod that was positioned $0.105''$ after region 2. Following supersonic expansion, the clusters passed through a 3-mm skimmer into the second differential region. The clusters were then ionized by $1+1'$ resonant two-color multiphoton ionization by crossing the jet with an unfocused pump beam consisting of both the residual fundamental and doubled fundamental of the appropriate laser dye wavelength (DCM, Rhodamine 640/610). The pump laser was the output of a dye laser (Quantel TDL-51) pumped by a Nd:YAG laser (Continuum NY-61) that was doubled to generate the UV beam (1-4 mJ/pulse). Figure 2a shows the ionization scheme employed. The clusters were scanned through the UV region from 330 nm to 296 nm, first exciting the Al atom $3p \rightarrow 3d$ transition with the doubled UV photon, and subsequently ionizing with the visible fundamental dye photon (10-50 mJ/pulse). In the current single dye laser

experiments, the UV and visible wavelengths ($\nu_{\text{vis}} = \frac{1}{2}\nu_{\text{UV}}$) were forced to tune simultaneously. The total photon energy ($\nu_{\text{UV}} + \nu_{\text{vis}}$) was always within 0.75 eV or less of the ionization threshold of the clusters.⁸

Following ionization, the clusters were extracted perpendicularly and mass-analyzed by a standard 1-m Wiley-McLaren time-of-flight (TOF) spectrometer, and detected by a microchannel plate. TOF mass spectra (Figure 2b) were collected by a transient digitizer (LeCroy 8818). Individual scans were recorded by gating the mass peak of interest with a gated integrator. S/N was greatly improved by switching the laser vaporization Q-switch at half the rep rate and using the gated integrator to subtract the pump background due to DP oil contaminant fragments (LV off) from every signal shot (LV on). All spectra were normalized for UV fluence.

C. RESULTS

All of the $\text{Al}(\text{Ar})_n$ clusters ($n = 4 - 54$) exhibited two broad principal transitions. We have tentatively assigned them as arising from the Al $3p \rightarrow 3d$ transitions. One band was blue-shifted relative to atomic Al $3p \rightarrow 3d$ transition (308.215 nm), and the other red-shifted.

The blue-shifted bands were generally broad and asymmetric. Figure 3 shows some typical spectra in the 305-297 nm region. For smaller clusters ($n \leq 12$), the peak shifted to the blue as n increased. However, a splitting was observed for larger clusters ($n \geq 18$). At $n = 18$, the peak was more symmetric and a dip started to appear at around 301 nm. The splitting became more pronounced as n increased.

The red-shifted bands were observed in the 325-308 nm region. Some typical spectra are shown in Figure 4. The peaks were also broad and asymmetric, but they showed a

monotonic increase in the red-shift relative to the atomic transition with cluster size (Figure 5). Moreover, the band positions varied in a stepwise fashion with n , and the changes appeared to coincide with the shell sizes ($n = 12$, and 54) for icosahedral shell closings.^{7,9} As shown in Figure 5, the peaks were close to 312 nm for $n \leq 12$, 320 nm for $25 \leq n \leq 40$, and 324 nm at $n = 54$. This result suggested that the observed spectral shifts indeed reflected the structural evolution in the clusters, and that cluster fragmentation was not seriously degrading the size-selectivity of our measurements.

D. DISCUSSION

The observed patterns in this experiment resulting from putative Al atom $3p \rightarrow 3d$ transitions as well as those observed by Whetten involving Al transitions between the $3p \rightarrow 4s$ differ significantly from the matrix features. Most notable is the difference in the magnitude of the cluster electronic band shifts relative to those of the matrix. The two resolved bands in the matrix appear at 291 nm and 286 nm have been assigned as $3p \rightarrow 3d$ transitions. In contrast, our R2MPI spectra of $\text{Al}(\text{Ar})_n$ ($n < 55$) exhibit a considerably less pronounced blue-shift. With small $\text{Al}(\text{Ar})_n$ clusters that form the first icosahedral shell ($n \leq 12$), a strong size dependent blue-shift is observed as the cluster size is monotonically increased (Figure 5). $\text{Al}(\text{Ar})_{12}$ shows a significant blue-shift maximum at 299 nm, but no splitting of electronic bands is observed. By $\text{Al}(\text{Ar})_{18}$ and for all larger clusters observed, the overall bandwidth and blue-shift remains roughly the same as for $\text{Al}(\text{Ar})_{12}$. However, by $\text{Al}(\text{Ar})_{18}$ a discernible splitting of the is evident. This splitting increases up to $\text{Al}(\text{Ar})_{34}$ at which point the splitting matches that in the matrix, namely 5 nm. Moreover, the dip between the bands remains at the same position for all clusters greater than $\text{Al}(\text{Ar})_{18}$. Hence, the increased splitting is due to equal red- and blue-shifts of the two respective

bands about the dip wavelength. This data suggests that the maximum blue-shift has been essentially achieved by $\text{Al}(\text{Ar})_{12}$, and that those interactions that give rise to the electronic band splitting are present by $\text{Al}(\text{Ar})_{34}$. However, the blue shifts are only about $+400\text{ cm}^{-1}$ and $+1100\text{ cm}^{-1}$ or $\sim 25\%$ and $\sim 44\%$ of the matrix shift, suggesting that even for the large clusters we have not been able to reproduce the bulk behavior.

Whetten and co-workers obtained analogous results in their R2MPI experiment on the $\text{Al}(\text{Ar})_n$ clusters ($n < 40$) $3p \rightarrow 4s$ transition.⁷ As was the case with the $3p \rightarrow 3d$ electronic bands, the $3p \rightarrow 4s$ band exhibited a strong monotonic blue-shift with increasing cluster size up to $\text{Al}(\text{Ar})_{12}$, after which the observed spectral shift leveled off. The maximum extent of the cluster $3p \rightarrow 4s$ blue-shift was $+700\text{ cm}^{-1}$, only 17% of the $+4200\text{ cm}^{-1}$ matrix shift. These shifts are proportionally smaller than those in the $3p \rightarrow 3d$ case. Such behavior caused Whetten to likewise conclude that these cluster systems do not yet resemble the bulk.

The other band observed during the course of this study in the wavelength range 330-310 nm has no assigned counterpart in any metal doped matrix study. These broad features are significantly red-shifted relative to the Al atom $3p \rightarrow 3d$ transitions. Similar to the blue-shifted putative $3p \rightarrow 3d$ $\text{Al}(\text{Ar})_n$ cluster bands, these red-shifted bands also exhibited a size dependence on the magnitude of the spectral shift. For the smaller clusters corresponding to the first icosahedral shell, the observed red-shifts were all small in magnitude relative to the Al atom $3p \rightarrow 3d$ transitions, and almost exactly the same as the red-shift in the $^2\Delta$ state of AlAr . Moreover, the spectral shifts in the first icosahedral shell did not evolve with increasing solvation. All cluster bands originating from the second icosahedral shell of the $\text{Al}(\text{Ar})_n$ clusters ($12 < n \leq 54$), are significantly red-shifted relative

to the first shell. A strong, monotonically increasing red-shift from 312 nm to 319 nm is observed in the cluster sizes $\text{Al}(\text{Ar})_{13}$ through $\text{Al}(\text{Ar})_{25}$. After $\text{Al}(\text{Ar})_{25}$, the cluster red-shift levels off for the rest of the clusters in the second icosahedral shell. Another significant red-shift to 324 nm is again observed upon complete solvation of the second shell.

An interesting question arises as to the nature of the structure in the $3p \rightarrow 3d$ case, as well as the origin of the cluster electronic splitting. In particular, it is puzzling that relatively small clusters like $\text{Al}(\text{Ar})_{34}$ can on one hand mimic the electronic band splitting of the bulk while on the other failing to achieve bulk characteristics such as the magnitude of the matrix blue-shift. If we examine the singly solvated system, namely AlAr , we find that there are three excited electronic states that arise from the $3d$ manifold that can be accessed by either $^2\Pi_{1/2}$ or $^2\Pi_{3/2}$ spin orbit ground state, namely $^2\Delta$, $^2\Pi$, and $^2\Sigma^+$. In AlAr , the $^2\Delta$ was observed to exhibit a significant red-shift relative to the Al atom transitions, while both the $^2\Pi$ and $^2\Sigma^+$ were slightly blue-shifted by less than 1 nm.¹⁰ The blue-shift of the $^2\Pi$ and $^2\Sigma^+$ states has been attributed to greater repulsive interactions in the excited state between Ar and the Al d_{xz} and d_{yz} for $^2\Pi$ and d_z^2 for $^2\Sigma^+$ (assuming z lies along the internuclear axis).[#] With respect to the $\text{AlAr } ^2\Delta$ state, the $d_{x^2-y^2}$ and d_{xy} orbitals lie perpendicular to the internuclear axis. The $^2\Delta$ red shift, then, can be attributed to the increase in Al atom polarizability upon excitation from the $3p$ to $3d$ orbitals.

The fact that the clusters in the first icosahedral shell exhibit almost the same red-shift as the $^2\Delta$ state in AlAr strongly suggests that this red-shifting band evolves from this state. The question arises, then, whether such a band is observable in the bulk matrix, or

[#] Due to uncertainty in the AlAr ground state D_0 value, the origin of the $^2\Pi$ blue shift is not definitive.

ultimately blue-shifts as $n \rightarrow \infty$. The other possibility could be that this red-shifted cluster band continues to red-shift in the matrix to form a $3d-4s$ hybrid band at the position currently assigned $3p \rightarrow 4s$ band position at 340 nm. Such a hybridization would be rather novel, but would further illuminate the intricacies involved in metal solvation.

While there is presently no single model that provides a complete interpretation of cluster structure based on the observed data, a potential candidate would place the Al atom always on or slightly above the outermost shell in a “cap site” (Figure 6). Evidence for such solute surface binding has been predicted by Alexander in a recent modified deterministic/stochastic genetic algorithm (DS-GA) study.¹¹ Alexander found that for the isoelectronic clusters, $B(Ar)_n$ ($n \leq 12$), the B atom prefers to lie on the surface of the cluster occupying a site with the fewest number of Ar nearest neighbors when the B-Ar interaction was described by both the attractive $^2\Pi$ state as well as the significantly more repulsive $^2\Sigma^+$ state. Due to similarities between the B-Ar and Al-Ar potentials, it would be reasonable to postulate that $Al(Ar)_n$ clusters may form similar structures.

The cap site model can account for many of the observed electronic band shift trends. In essence, the cap site model preserves much of the same bonding interactions as those of $AlAr$ itself. Therefore, the furthest blue-shifted band can be envisioned as arising from strong repulsive interaction between the d_z^2 of the Al atom and the cluster. Likewise, the d_{xz} and d_{yz} of the Al atom would be forced to orient into the Ar-Ar bonds that form the cap site, resulting in a lesser but still significant repulsive interaction that drives the band to the blue. Moreover, the observed red-shifting behavior of the putative $^2\Delta$ band can be justified by the cap site model. By occupying a cap site, the Al atom can minimize repulsive interactions between its $d_{x^2-y^2}$ and d_{xy} orbitals while at the same time stabilizing

the these orbitals by favorable π -type interactions with the Ar-Ar bonds that form the edges of the cap site.

A definitive interpretation of the current results requires accurate calculations addressing the cluster structure as well as the shifts and splittings of the electronic transitions as a function of cluster size. The $\text{Al}(\text{Ar})_n$ clusters should serve as important prototypes for metal-doped solids, and will provide a critical test of theoretical efforts to model these HEDM materials.^{4,12}

E. REFERENCES

- ¹ *Proceedings of the High Energy Density Materials (HEDM) Conference*, edited by P. G. Carrick and S. Tam (Phillips Laboratory, Edwards AFB, CA, 1996).
- ² H. Abe and D. M. Kolb, *Ber. Bunsenges. Phys. Chem.*, **87**, 523-527 (1983).
- ³ R. Grinter and R. J. Singer, *Chem. Phys.*, **113**, 87-97 (1987).
- ⁴ M. E. Fajardo, S. Tam, T. L. Thompson and M. E. Cordonnier, *Chem. Phys.*, **189**, 351-365 (1994); J. A. Boatz and M. E. Fajardo, *J. Chem. Phys.*, **101**, 3472-3487 (1994); R. A. Corbin and M. E. Fajardo, *J. Chem. Phys.*, **101**, 2678-2683 (1994); S. Tam and M. E. Fajardo, *J. Chem. Phys.*, **99**, 854-860 (1993); M. E. Fajardo, *J. Chem. Phys.*, **98**, 119-125 (1993); M. E. Fajardo, *J. Chem. Phys.*, **98**, 110-118 (1993); M. E. Fajardo, P. G. Carrick and J. W. Kenney, *J. Chem. Phys.*, **94**, 5182-5825 (1991).
- ⁵ F. Stienkemeier, J. Higgins, W. E. Ernst, and G. Scoles, *Z. Phys. B*, **98**, 413-416 (1995), and references therein.
- ⁶ A. I. Krylov, R. B. Gerber, M. A. Gaveau, J. M. Mestdagh, B. Schilling, and J. P. Visticot, *J. Chem. Phys.*, **104**, 3651-3663 (1996), and references therein.
- ⁷ R. L. Whetten, K. E. Schriver, J. L. Persson and M. Y. Hahn, *J. Chem. Soc. Faraday Trans.*, **86**, 2375-2385 (1990).
- ⁸ K. E. Schriver, M. Y. Hahn, J. L. Persson, M. E. LaVilla and R. L. Whetten, *J. Phys. Chem.* **93**, 2869-2871 (1989).
- ⁹ D. A. Estrin, L. Liu and S. J. Singer, *J. Phys. Chem.*, **96**, 5325-5331 (1992).
- ¹⁰ S. A. Heidecke, Z. Fu, J. R. Colt, and M. D. Morse, *J. Chem. Phys.*, **97**, 1692-1710 (1992).
- ¹¹ S. K. Gregurick, B. Hartke, and M. H. Alexander, *J. Chem. Phys.*, **104**, 2684-2691 (1996).
- ¹² P. W. Langhoff, *J. Phys. Chem.*, **100**, 2974-2984 (1996).

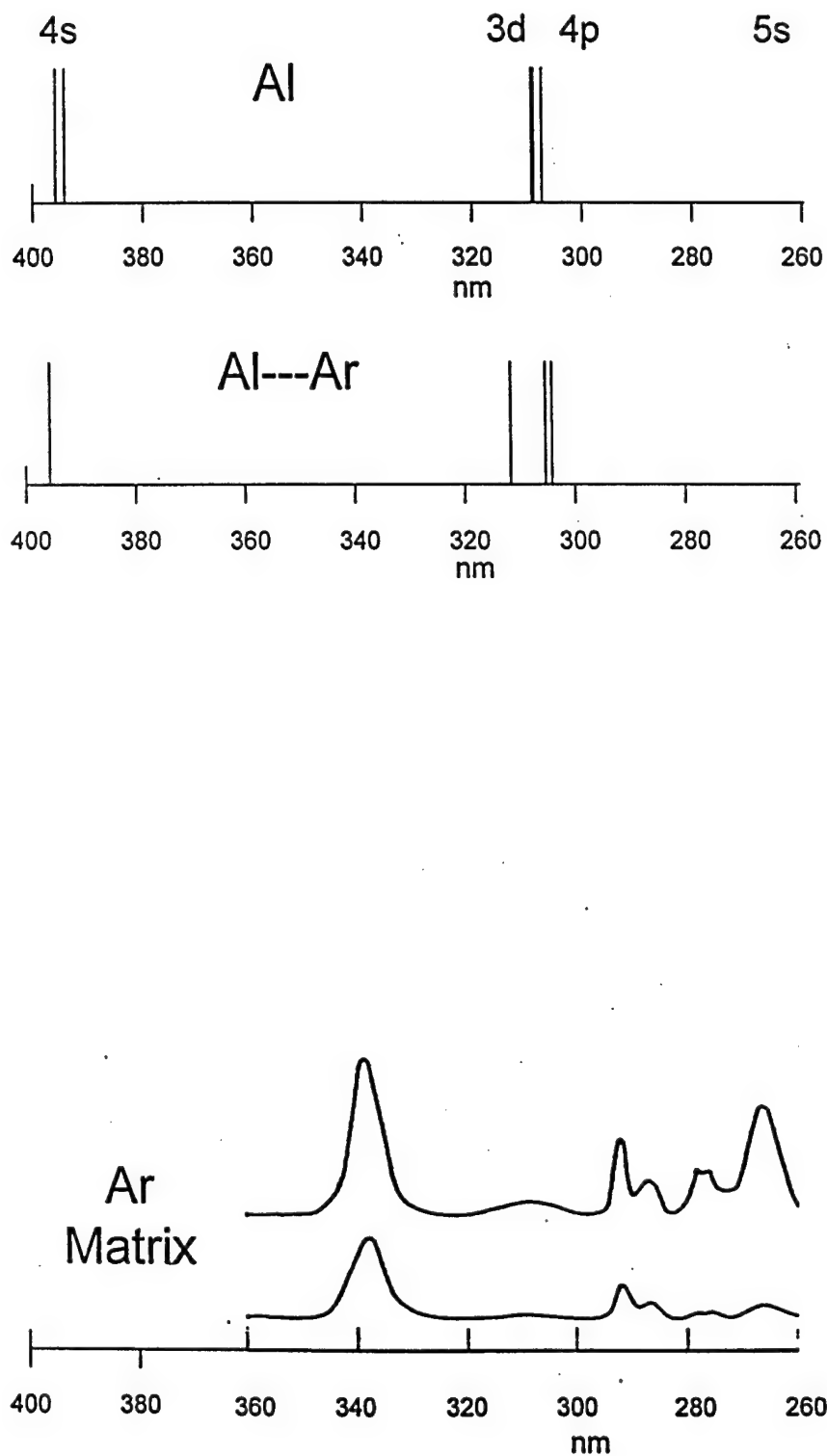


Figure 1. Upper: Absorption lines of Al Atom. Middle: Band origins of AlAr. Lower: Absorption spectrum of Al atoms doped in Ar matrix.

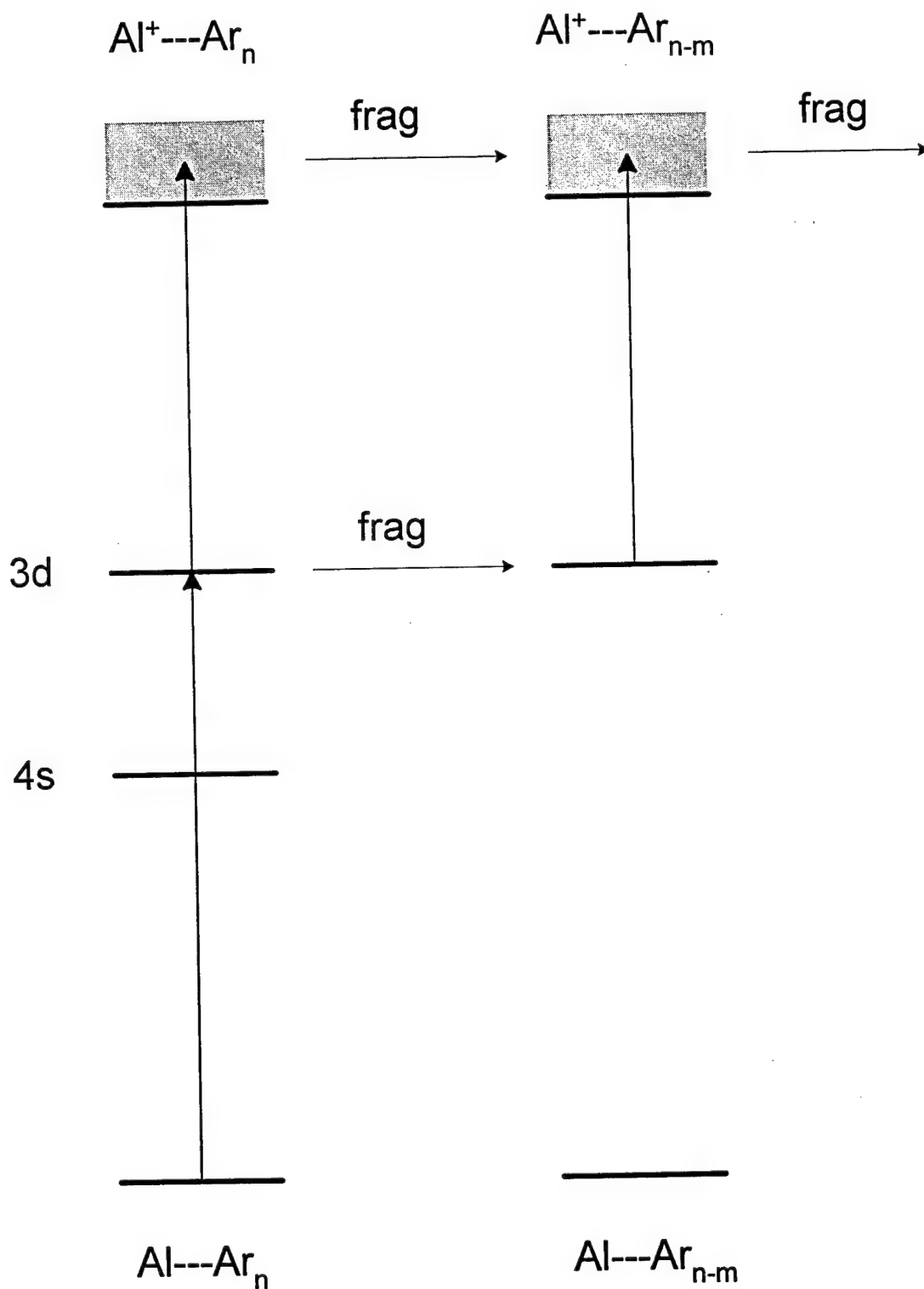


Figure 2a. Resonant two photon ionization scheme for AlAr_n clusters, including possible fragmentation pathways.

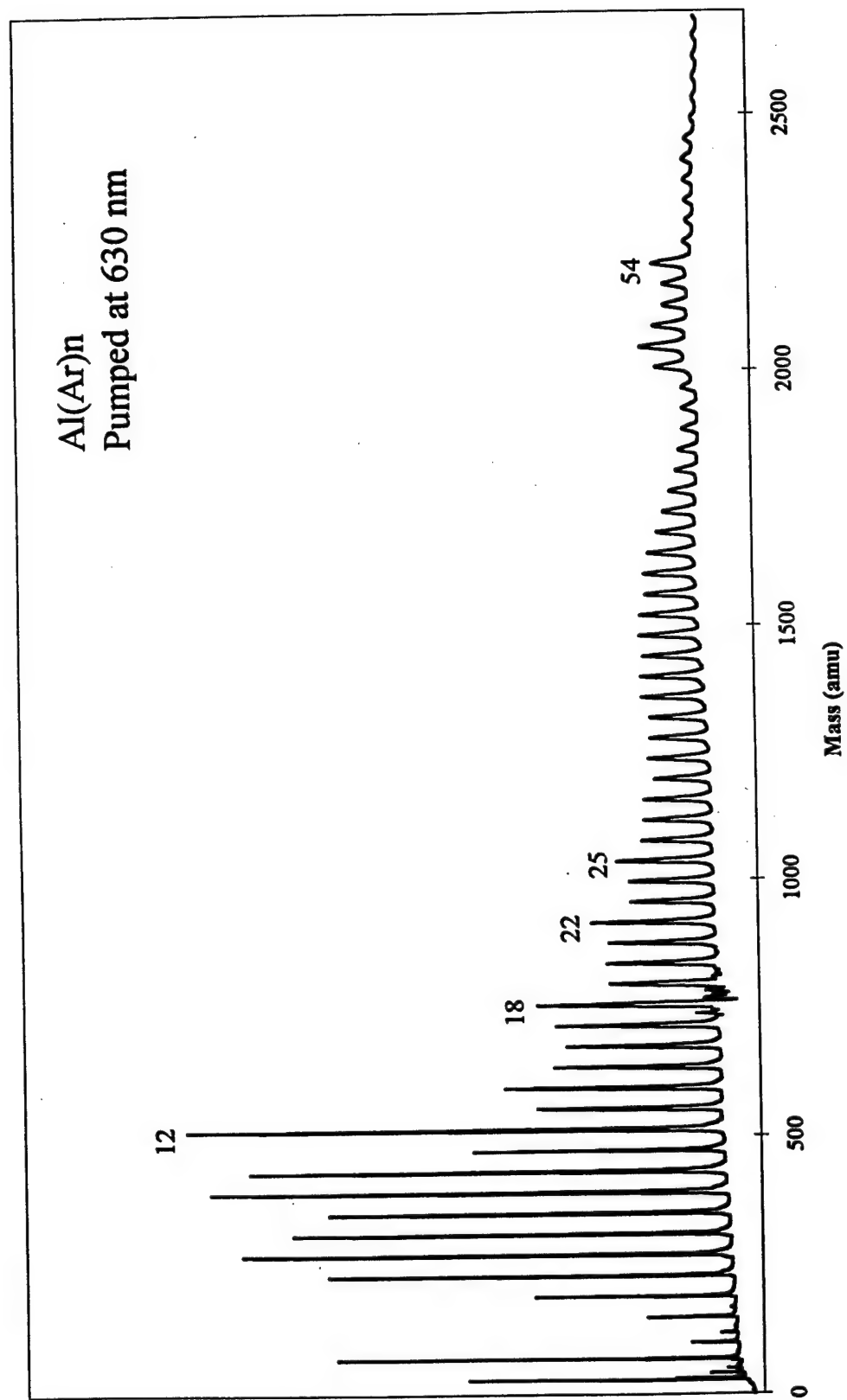


Figure 2b. Typical AlAr_n photoionization mass spectrum.

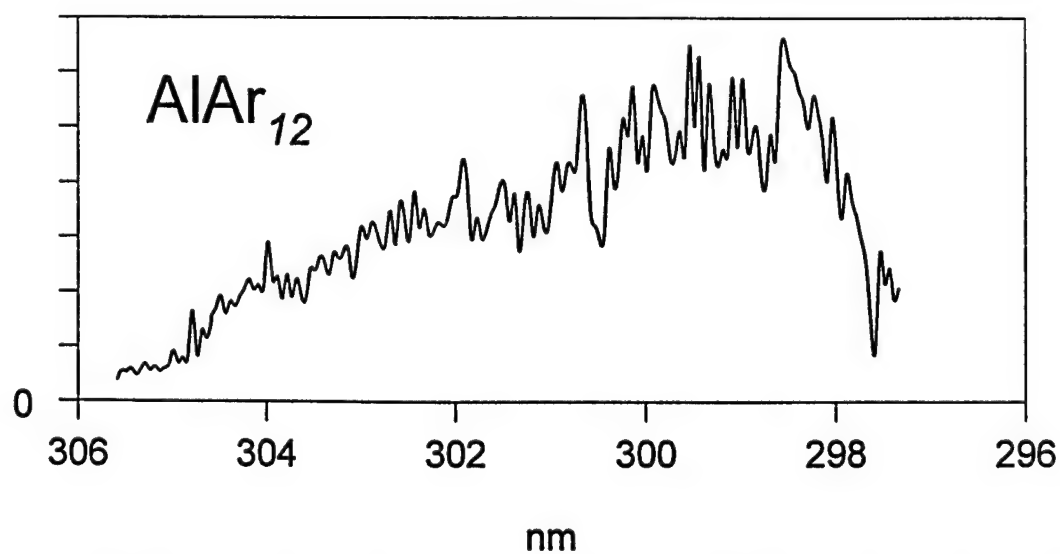
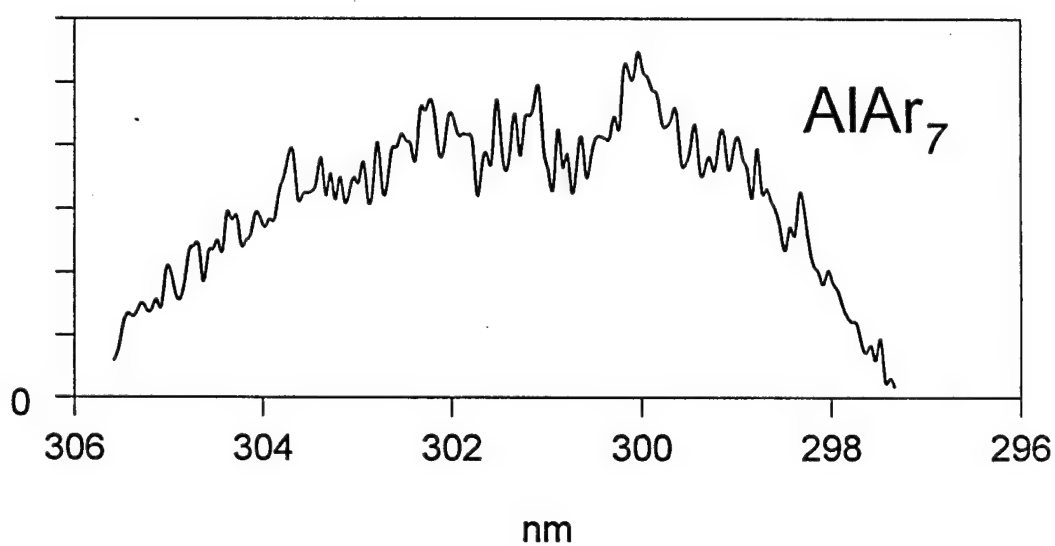
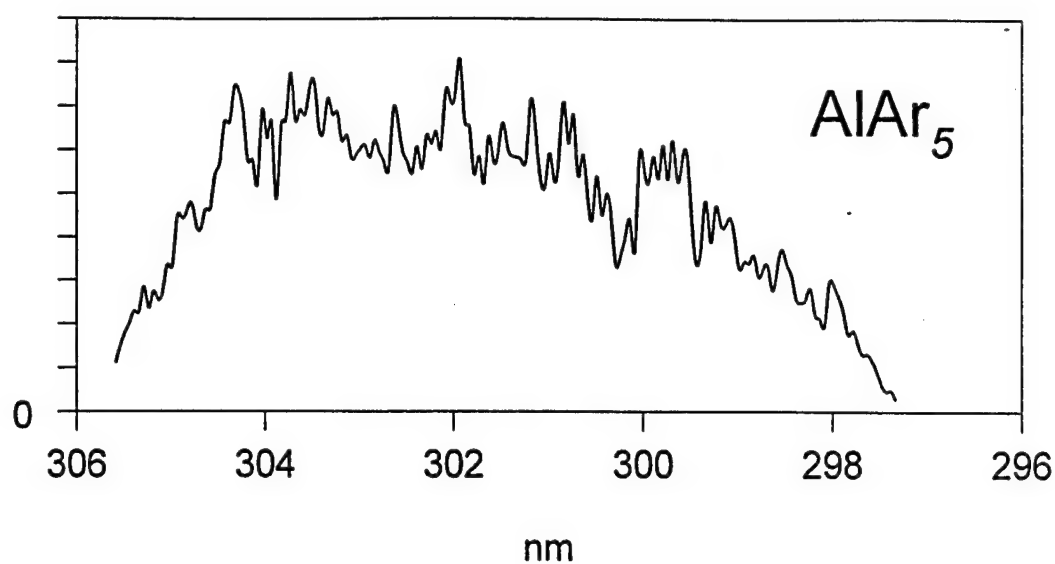


Figure 3. Absorption spectra taken by R2MPI of some AlAr_n clusters.

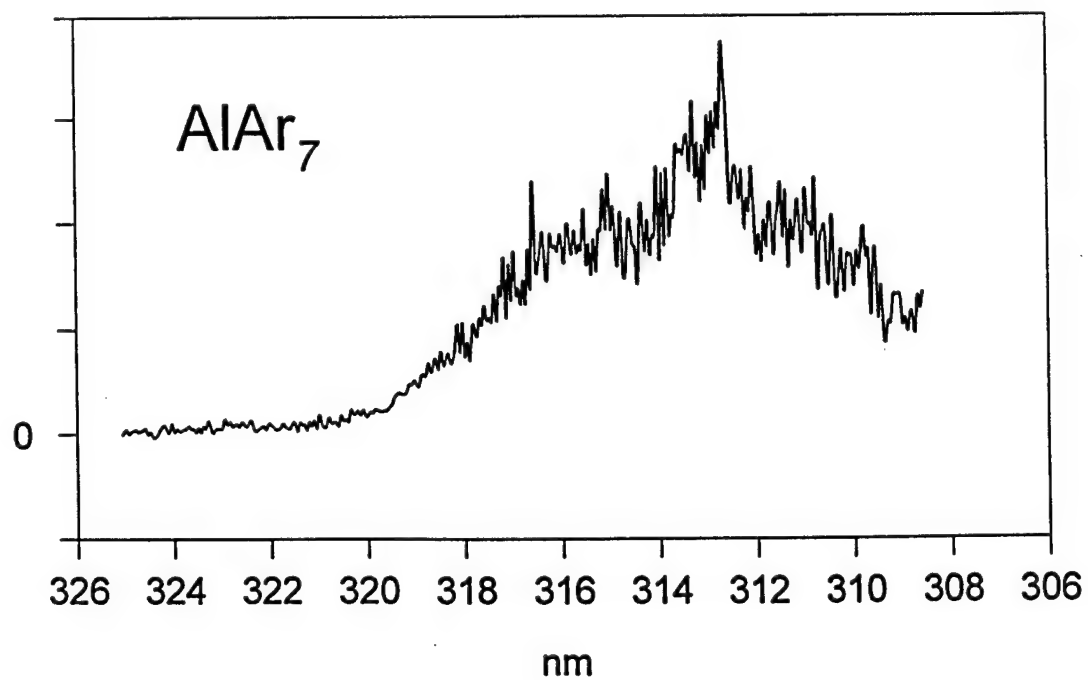
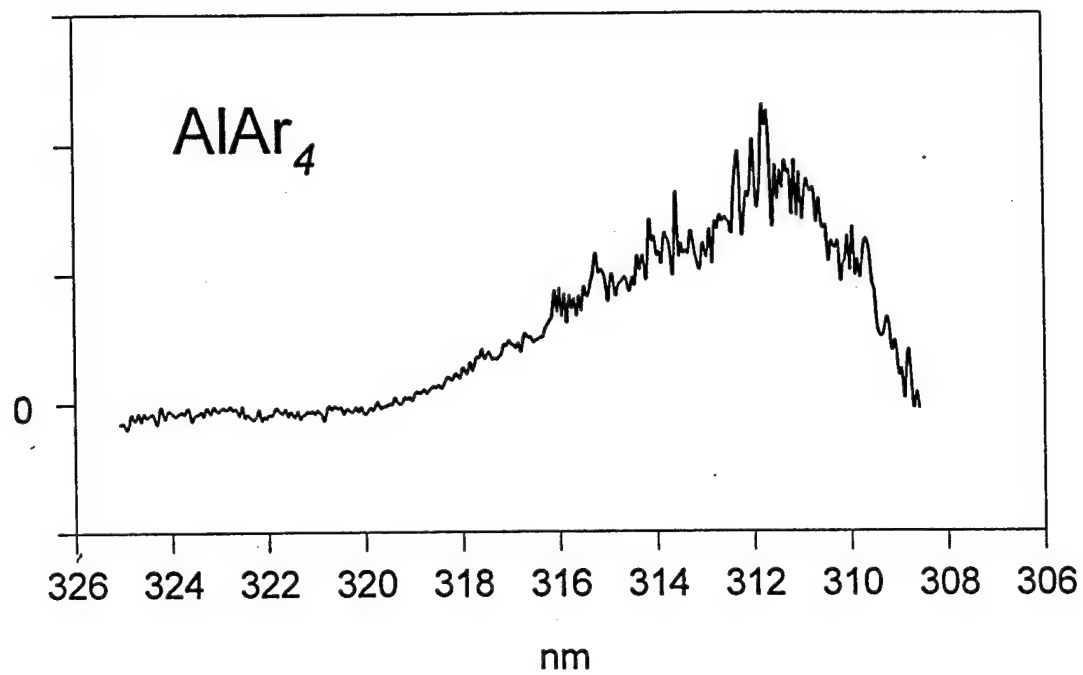


Figure 4a. R2PI spectra of AlAr_n , $n=4,7$.

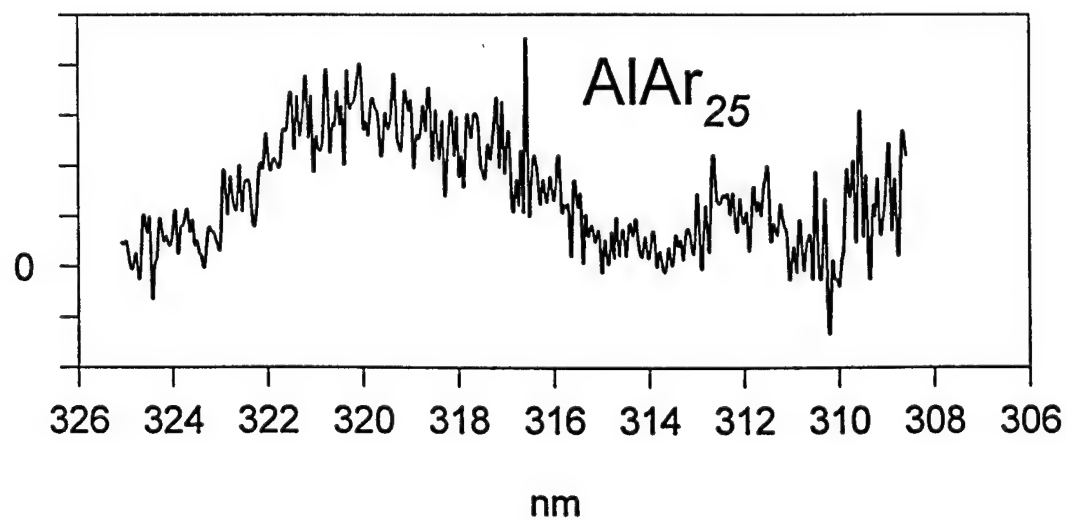
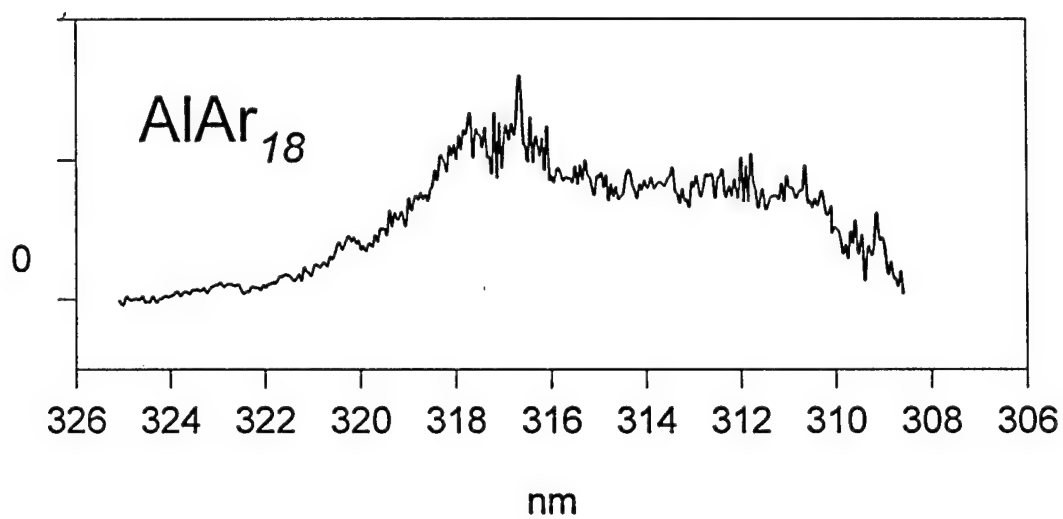
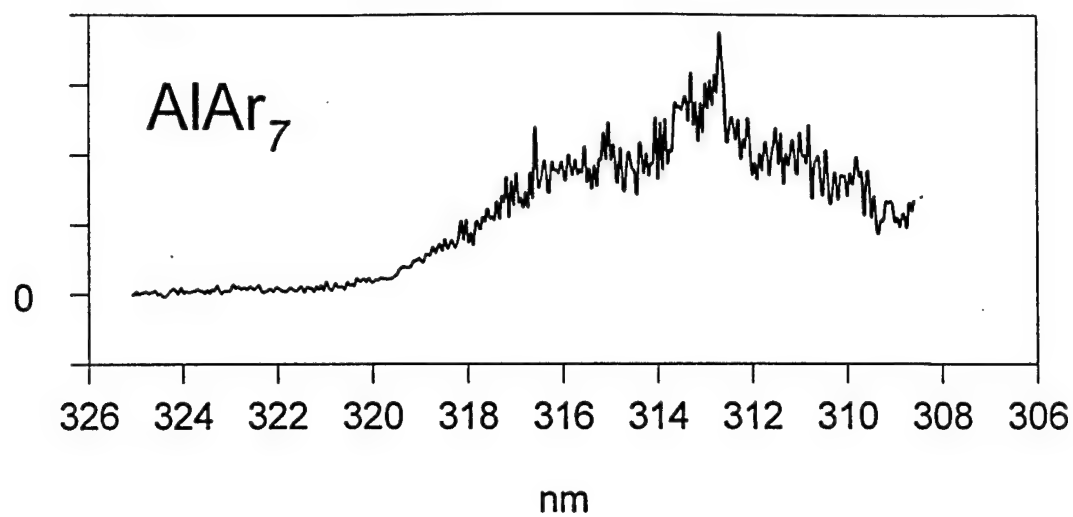


Figure 4b. R2PI spectra of AlAr_n, n=7,18, and 25.

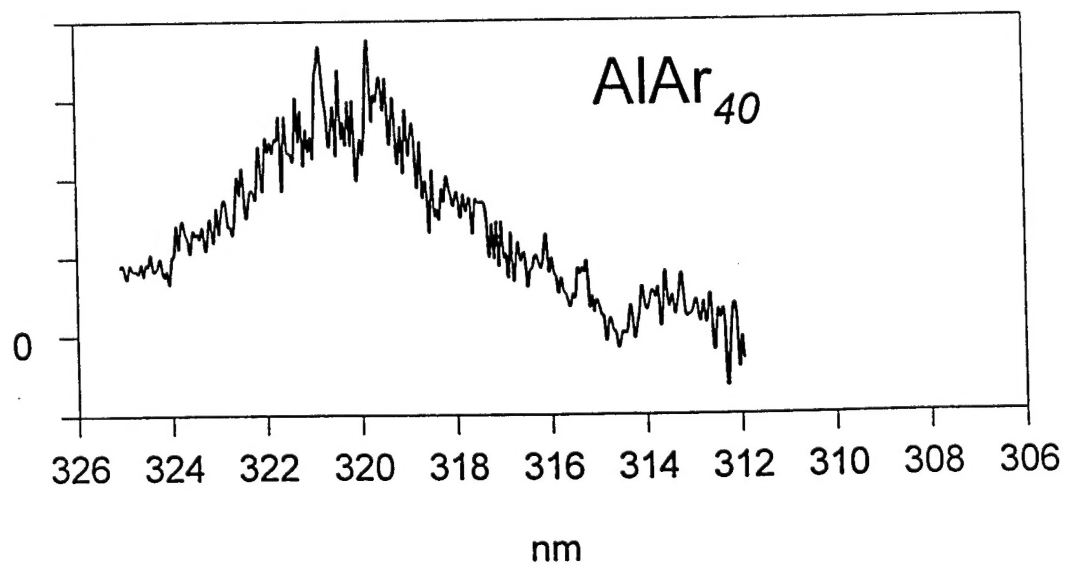
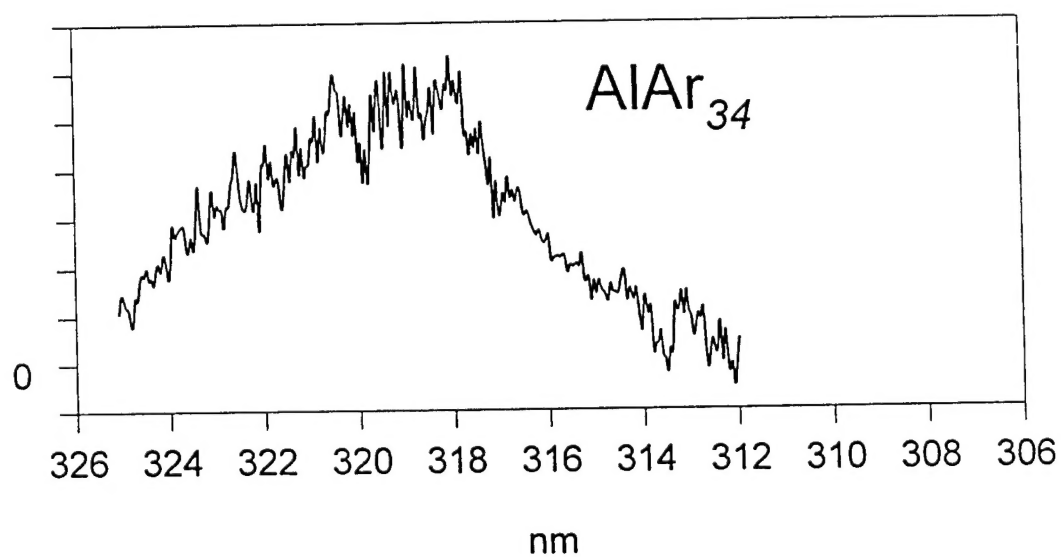
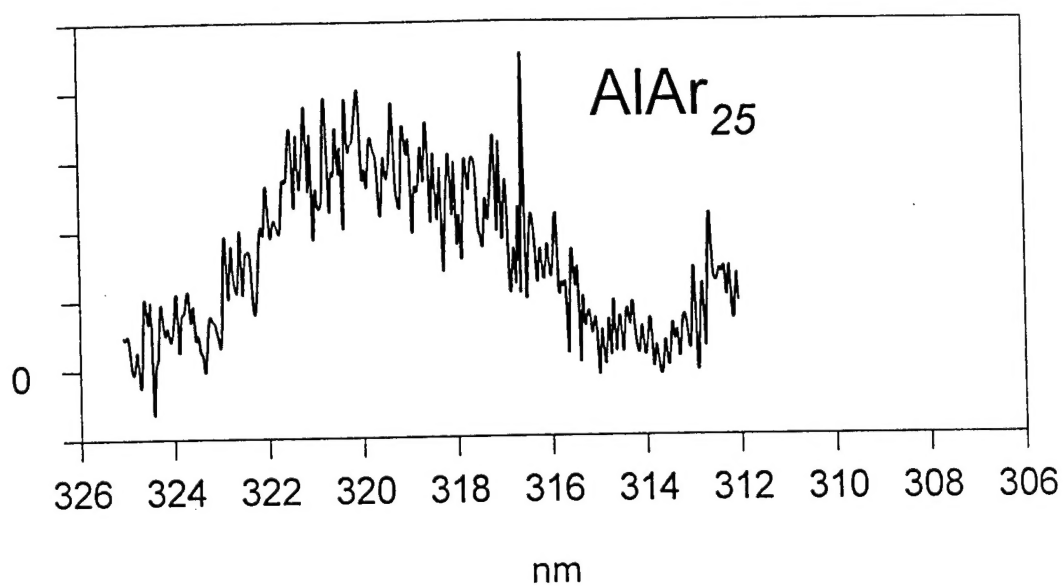


Figure 4c. R2PI spectra of AlAr_n , $n = 25, 34$, and 40 .

3p-3d Band Positions of AlAr_n

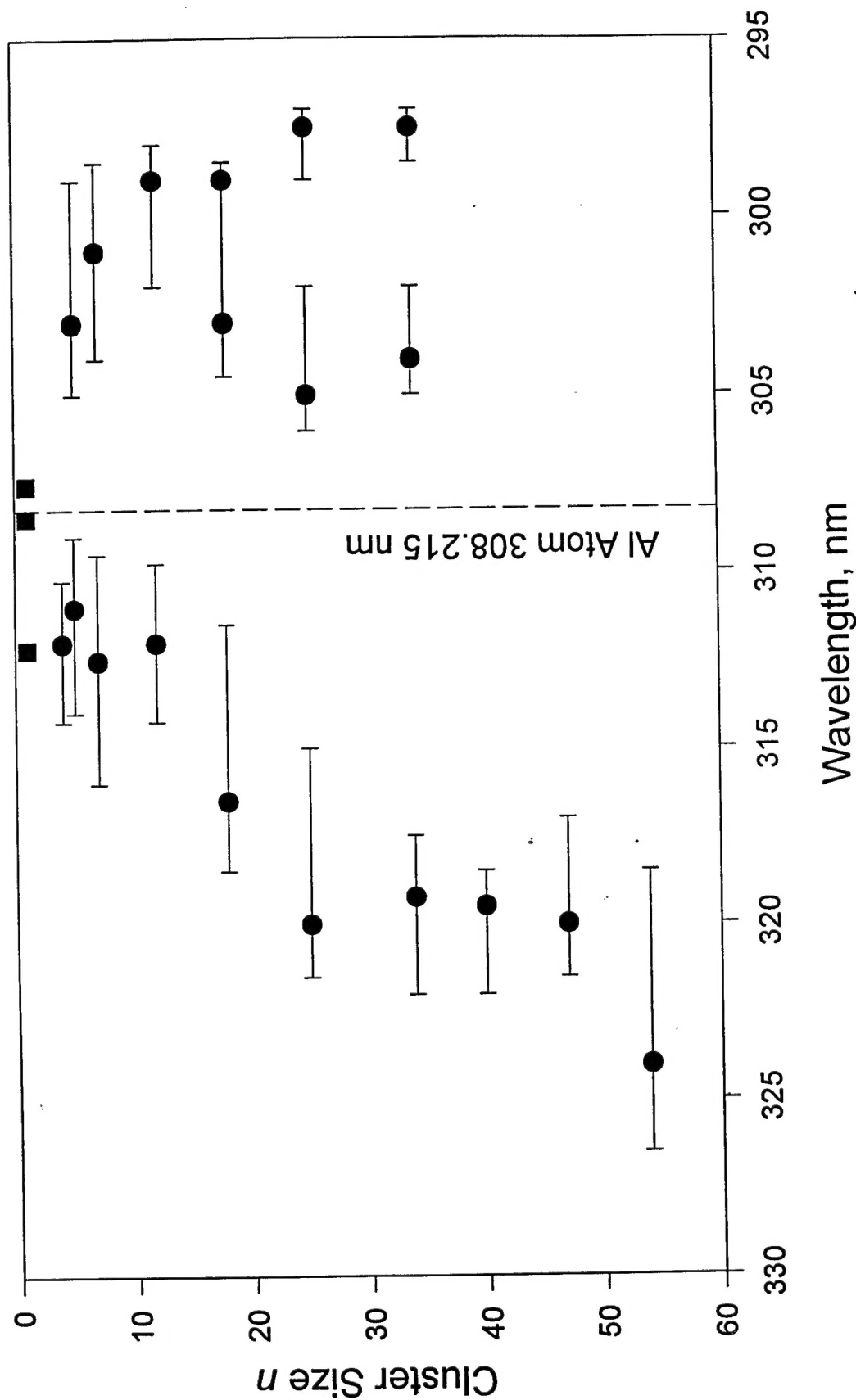


Figure5. Band positions and widths (bars) for AlAr_n transitions as a function of cluster size.

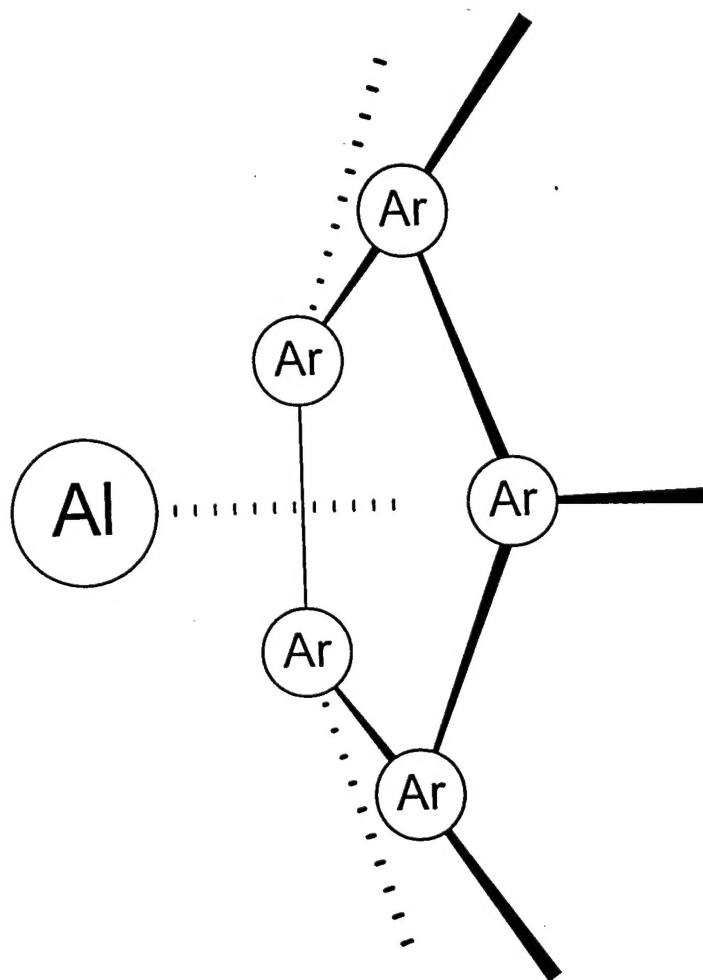


Figure 6. Hypothetical "cap" model structure with Al atom capping face of an Ar_n cluster.

IV. Laser-Induced Fluorescence Spectroscopy of AlNe

Spectra of AlNe complexes (see Figure 1 below) were obtained by expanding pure Ne through the laser vaporization source at stagnation pressures of 1-3 bar. Eight bands were observed between 312.6 and 309 nm. Although the origin was not found, from these bands we estimate that the vibrational parameters for the upper state are

$$w_e \approx 51 \text{ cm}^{-1}$$

$$w_e x_e \approx 1 \text{ cm}^{-1}$$

$$D_0 \approx 650 \text{ cm}^{-1}$$

The band position, to the red of the Al atom $3p \rightarrow 3d$ transition, suggests that this band should be assigned to the $X 3p^2\Pi_{1/2} \rightarrow 3d^2\Delta$ transition of AlNe. The force constants are comparable to the analogous state in AlAr.

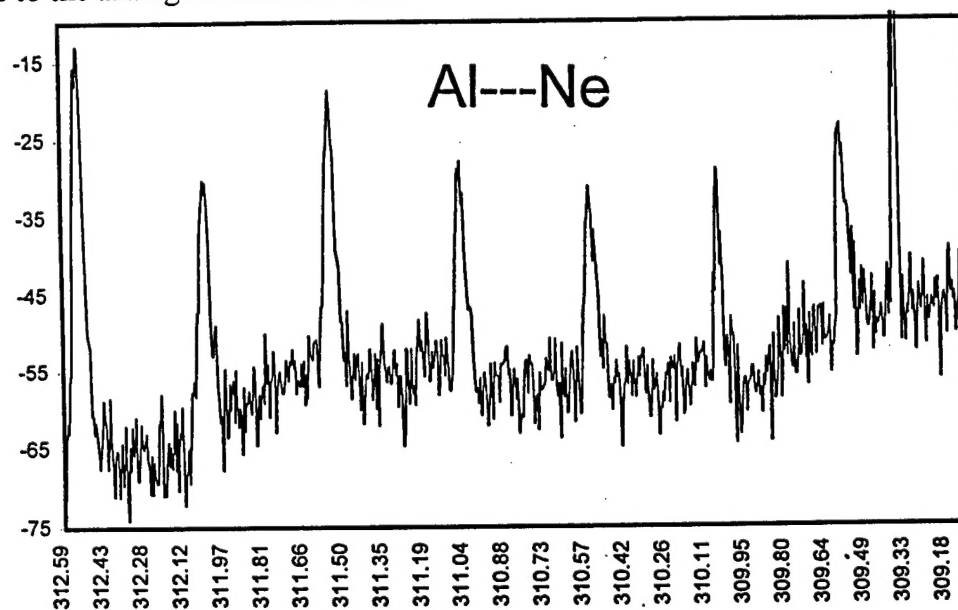


Figure 1. Observed LIF spectrum of AlNe.